Tunable Metamaterials for Controlling THz Radiation

Irina B. Vendik, *Senior Member, IEEE*, Orest G. Vendik, *Senior Member, IEEE*, Mikhail A. Odit, Dmitry V. Kholodnyak, Svetlana P. Zubko, *Member, IEEE*, Margarita F. Sitnikova, *Member, IEEE*, Pavel A. Turalchuk, Kirill N. Zemlyakov, Irina V. Munina, Dmitry S. Kozlov, Viacheslav M. Turgaliev, Alexey B. Ustinov, Yeonsang Park, Jinyun Kihm, and Chang-Won Lee

***Abstract*—Remarkable progress in terahertz (THz) sources and detectors is followed by the necessity of manipulating of terahertz radiation. Since natural materials can not perform efficient interaction with THz radiation, artificial structures called metamaterials are designed to overcome "THz gap" in this area. A variety of tunable metamaterials using different methods of control are presented and discussed in this review paper.**

***Index Terms*—Terahertz (THz), tunable metamaterial.**

I. Introduction

TERAHERTZ science and technology became recently attractive due to potential new applications such as terahertz imaging/sensing [1], medical scanning, security screening, quality control, atmospheric investigation, space research, etc. [2]. As compared to the microwave electronic and optical photonic technologies, the development of THz technology is lagging far behind, because the THz spectral region has difficulty in exploring due to the lack of appropriate and effective sources and detectors. In addition, natural materials do not exhibit strong magnetic or electric responses in the THz frequency range, for example, 1–3 THz. The resonant response of conventional magnetic materials occurs at microwave frequencies, while the plasma frequency in natural metals is observed beyond the mid-infrared range. So in the THz frequency range there is a lack of natural materials exhibiting magnetic or electric responses. This lack of the natural materials is considered as the THz frequency gap. New types of materials should be searched in order to cover this gap and to keep the progress of THz research by tailoring new artificial materials. Among novel materials, artificially structured materials play an important role particularly in the design of functional THz devices. The new artificial materials known as electromagnetic metamaterials (MTM) have been actively studied to enhance desired electromagnetic properties in any frequency range. The metamaterials can complete the THz frequency gap and stimulate the terahertz research and development. Electromagnetic MTM have enabled numerous exotic electromagnetic phenomena, such as negative or zero dielectric permittivity, negative or zero magnetic permeability, double-negative refractive index, perfect lensing, cloaking etc [3], [4]. The metamaterials are expected to cover the niche for THz manipulating devices, which is not possible with conventional materials. The THz spectrum represents a fascinating arena for metamaterial research.

Fabricating metamaterials for THz spectrum is a challenging task. The metamaterial structure is usually arranged as a regular array of unit cells. The size of the unit cell for THz region is scaled to micrometers or even hundreds of nanometers in comparison with millimeters for microwave region. Even though there is a big challenge to manipulate THz radiation at desired way, functional devices such as filters, switches, modulators, phase-shifting and beam-steering devices for THz electromagnetic spectrum are now being investigated. Also, tunable or controllable THz devices are soon to promise the practical applications working in THz spectrum by constructing controllable metamaterials. In this philosophy, we have analyzed a number of published articles related to the tunable THz metamaterials. In this review, we categorize approaches to design tunable MTM for THz applications in the following way:

— MTM based on split-ring resonators;
— MTM based on dielectric resonant inclusions;
— ferroelectrics and ferromagnetic based MTM;
— MTM based on phase change materials;
— layered metal-dielectric structures of MTM;
— MTM infiltrated with liquid crystals.

II. Controllable Metamaterials

A. MTM Based on Split-Ring Resonators (SRR)

Electromagnetic MTM typically consist of sub-wavelength metallic resonator arrays fabricated on dielectric or semiconductor substrates, which collectively respond to either or both the magnetic and electric components of the incident electromagnetic field. By proper scaling, MTM properties have been demonstrated from radio to near visible frequencies. A key component of many MTM structures is metallic resonator. Most popular form of a canonical "metaparticle" is the split-ring resonator (SRR) and its modifications. The SRR was introduced theoretically by Pendry in 1999 [5] and experimentally verified by Smith *et al.* in 2000 [6]. The SRR was originally designed and utilized for a magnetic response. As shown in Fig. 1, when a time varying magnetic field is polarized normal to the plane of the SRR, the circulating current will be induced within the ring, resulting in a negative magnetic response above the resonant frequency. SRR can also be used as an electrically resonant

Manuscript received April 24, 2012; accepted July 09, 2012. Date of publication August 27, 2012; date of current version August 30, 2012. This work was supported by Samsung Electronics Company.

I. B. Vendik, O. G. Vendik, M. A. Odit, D. V. Kholodnyak, S. P. Zubko, M. F. Sitnikova, P. A. Turalchuk, K. N. Zemlyakov, I. V. Munina, D. S. Kozlov, V. M. Turgaliev, and A. B. Ustinov are with the St. Petersburg Electrotechnical University "LETI," 197376 St. Petersburg, Russia (e-mail: ibvendik@rambler.ru).

Y. Park, J. Kihm, and C.-W. Lee are with the Samsung Advanced Institute of Technology, Giheung-Gu, Yongin-Si, 449-712, Korea (e-mail: chang-won.lee@samsung.com).

Color versions of one or more of the figures in this paper are available online at http://ieeexplore.ieee.org.

Digital Object Identifier 10.1109/TTHZ.2012.2209878

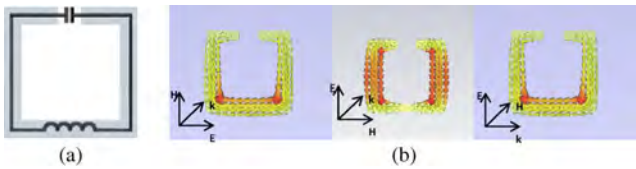

Fig. 1. (a) Equivalent diagram of a single SRR, (b) different types of excitation and corresponding current distribution along the SRR structure.

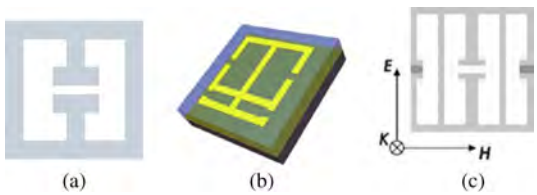

Fig. 2. Sample of (a) a single-band electric SRR (eSRR) [8] and (b) dual-band ELC resonator [9]. (c) A novel version of ELC resonator from [15].

unit as it exhibits a strong resonant permittivity at the same frequency as the magnetic resonance by 90° rotating the incident THz radiation with the electric field perpendicular to the gap and the magnetic field lying completely in the SRR plane.

The SRR can be presented as an equivalent LC resonant circuit (Fig. 1(a)). The resonance frequency of the SRR can be calculated by $\omega_0 = \sqrt{1/LC}$, where the inductance L results from the current path of the SRR and the capacitance C is determined by the gap dimensions.

In general, both the material and the structure of the MTM unit cell determine their electromagnetic characteristics. In order to avoid unwanted electromagnetic characteristics associated with a periodic structure, the dimensions of the unit cell of MTM should be smaller than the wavelength λ_0 at the operating frequency. For frequencies in range of 100–1000 GHz, the linear size of the SRR should be compared with micrometer or even hundreds nanometers.

Recent progress in MTM design has led to the realization of frequency-agile functionality provided by a tunability of metamaterials. In order to achieve agility of the operating frequency, external stimulus-dependent tunable elements are necessary to be incorporated into the designs for altering L and/or C. For that purpose, modifying the dielectric properties of the SRR and/or the substrate to modify the inductance and/or capacitance are used. The most efficient methods are the following: micromechanical, thermal, optical, electrical, and magnetic control.

A variety of SRR modifications and combinations of SRR with other constituents of the MTM array have been considered in [7]. The example of electric split-ring resonator (eSRR) is shown in Fig. 2(a) [8]. This configuration was used in [9] for stacking multiple single-layer planar metamaterials fabricated on thin, flexible polyimide substrates. Excitation of the inductive-capacitive (LC) resonance of the eSRR arrays evolves into a full band-stop transmission centered at the resonance frequency. Using the elementary cell of Fig. 2(b), the dual band absorber consisting of a dual band electric-field-coupled (ELC) resonators and a metallic ground plane, separated by a dielectric spacer was proposed in [10].

Metamaterials with **micromechanical** control of SRR is based on utilizing **bimaterial** cantilever. In [11], a method of

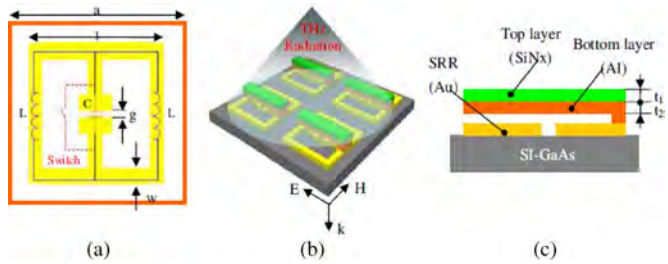

Fig. 3. The single cell of the MTM consists of two single SRRs put together on the split gap side with a cantilever sitting above [11]. (a) Equivalent circuit of the single cell of the THz MTM resonant switch; (b) planar periodic array exposed to normal incident THz radiation with electric field directed along the SRR gap; and (c) cross-sectional view of one individual element.

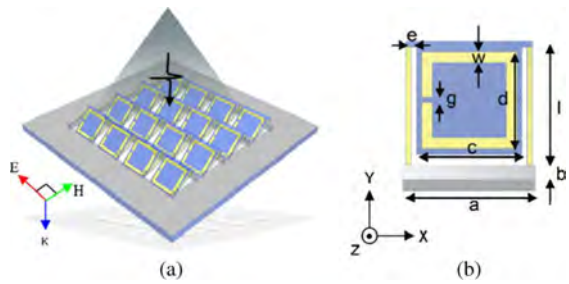

Fig. 4. (a) Schematic of structurally tunable THz MTM and (b) dimensions of a single SRR unit cell [12].

the dynamical control of the resonant electrical response of the THz MTM was reported (Fig. 3). The design approach is based on a planar array of eSRRs manufactured by microfabrication methods to create a biomaterial cantilever based THz MTM switch with the cantilever sitting above the gap, which operates by modifying or shorting the SRR capacitive gap. The MTM element interacts strongly with a uniform electric field, and weakly with a uniform magnetic field. The effective LC resonance results in a frequency dependent transmission, where, on resonance, a strongly enhanced electric field is concentrated in the gap of the SRR. Therefore, the resonance disappears when the cantilever bends down to touch the SRR and shorts the gap. The switch operates by controlling the ambient temperature to make the bimaterial cantilevers bend up due to the different thermal expansion of Al and SiN_x.

It is known that the resonant response of the MTM depends also on the coupling efficiency of the SRR to electromagnetic field. It was suggested in [12] to rotate individual "meta-atoms" to tune the EM field coupling efficiency while keeping the sample plane normal to the incident wave. This is accomplished by fabricating planar arrays of SRRs on **bimaterial cantilevers** designed to "pop-up" out of plane in response to a thermal stimulus, as shown in Fig. 4. There are 4 possible responses, demonstrated by that agile structure: (a) pure tunable electrically resonant response; (b) pure tunable magnetically resonant response; (c) bianisotroic response; and (d) nonresonant response.

Another method of controlling metamaterial transmission response is to introduce **MEMS devices** into the structure [12], [13]. The MTM unit cell of the THz tunable MTM filter [13] is tuned by micromachined comb-drive. The MTM slab works as a notch filter in THz region. Each unit cell consists of two

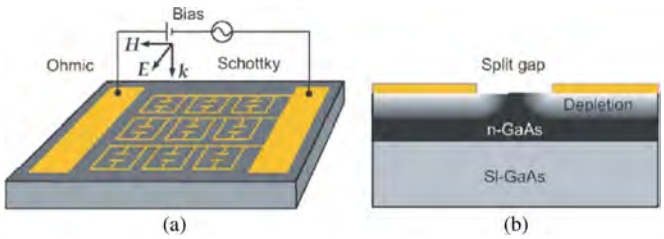

Fig. 5. Electrically controlled terahertz modulator [16]. (a) A layout showing an array of planar eSRRs, biasing pads, external electric circuit, and exciting terahertz field. The eSRRs form a Schottky contact with the substrate. (b) A cutaway view reveals a build-up of the depletion region underneath the metal as a result of the reversely biased Schottky junction.

split semi-squares. One semi-square is located on the thin silicon rib, which can be moved by the MEMS comb-drive. The other semi-square is located on the thick silicon island which is fixed at all time. The gap of the two semi-squares is controlled by the pump voltage of the comb-drive providing tunability of the filter.

The tunable metamaterials based on SRRs on semiconductor substrate with variable conductivity are considered in [14]–[17]. **Thermal control** is based on a variation of temperature altering the intrinsic carrier density in a semiconductor (InSb) [12]. By integrating semiconductors into metamaterial designs, **photoexcitation** is used for the MTM control. In [15], a design for blueshift tunability with a photoconductive semiconductor incorporated into the metamaterial was presented. This approach takes advantage of a novel version of the ELC resonator [see Fig. 2(c)]. It was shown that the tuning can be implemented within quite a broad frequency range of as much as $\sim$40% and is achieved through an effect of photoconductivity-induced mode switching. The controllable unit cell was designed by inserting photoconductive silicon within the two side gaps but not the central gap of the combined ELC resonator placed on a thick sapphire substrate. From the field and current distribution for cases without illumination $\sigma_{\mathrm{Si}} = 1$ S/m and with heavy photodoping $\sigma_{\mathrm{Si}} = 50\,000$ S/m at their respective resonance frequencies. Obviously, the resonances of the two cases belong to very different modes, so the blueshift of the resonance frequency can be considered to be due to a photoconductivity-induced mode-switching effect.

In [16], the same idea of photoexcitation, that later was patented [17], is used. A series of novel planar electric metamaterials operating at THz frequencies was created. High efficiency, all-electronic THz switching and modulation operating at room temperature have been accomplished by the use of a **hybrid of metamaterial and Schottky diode structure** (see Fig. 5). Dynamic switching of THz radiation was achieved by photoexcitation of the semiconductor substrate, where ultrafast switching has been demonstrated by the use of an ErAs/GaAs nano-island superlattice substrate.

To achieve switching behavior, the unit cell similar to that shown in Fig. 2(a) was used. Metallic SRRs were patterned to form a square array and connected by metal wires. They were fabricated on a 1-mm-thick epitaxial n-doped GaAs layer with the electron density of $2 \cdot 10^{16}$ cm^{-3} grown on an undoped GaAs wafer [16]. The metal–semiconductor interface forms a Schottky diode structure as shown in Fig. 5. The depletion regions underneath and around the metal, particularly near the split gaps, can be actively controlled by applying a voltage bias between the metal and substrate.

The control of the conductivity of the substrate near the split gaps can be effectively implemented, which in turn switches the resonance of the eSRR. With no voltage bias the metamaterial resonance response is strongly damped due to the conducting and lossy substrate, i.e., the split gaps of eSRRs are shortened by the relatively conducting substrate. A reverse voltage bias, on the other hand, drives electrons away from the interface and increases the width of depletion regions. This isolates the metal from the doped semiconductor substrate, and particularly, recovers the split gaps.

The dynamic switching off of the MTM resonance response can be very fast, i.e., only depending on the femtosecond photoexcitation of charge carriers. The switching recovery time, however, is determined by the carrier lifetime.

B. MTM Based on Dielectric Resonant Inclusions

In order to avoid conducting loss in metal elements of traditional metamaterial designs (SRR or wire medium), MTM structures based on low loss dielectric resonators were introduced. Nowadays there is a plenty of different structures of metamaterials utilizing Mie resonances [18] in dielectric particles. The Mie resonances of dielectric inclusions provide magnetic or electric response based on displacement currents, and offer a simpler and more versatile route for the fabrication of isotropic metamaterials operating at higher frequencies.

The all-dielectric metamaterial consists of dielectric particles only and provides single-negative (SN) or double-negative (DNG) properties. High permittivity dielectric spheres, cubes or rods are usually used to observe the negative effective permeability [19]–[21]. Negative permittivity can be obtained by adding conducting wires into the structure [22], [23].

Spherical dielectric resonators based MTM structures open up the possibility of fabricating homogeneous and isotropic negative refractive index metamaterials. The idea of a design of all-dielectric DNG metamaterials was suggested in [24] and further developed in [25], [26]. The MTM is formed as an array of spheres of different diameters with magnetic and electric resonances corresponding to magnetic and electric dipoles providing effective negative permeability and permittivity. Advancing all-dielectric MTM towards the THz frequency range is provided by scaling procedure while using the MTM particles of smaller dimensions. The scaling procedure is limited by existence of the intrinsic dispersion of materials used for the tunable MTM design. For example, the resonance in ferromagnetic and ferroelectric materials is observed in a limited frequency range, where the properties of the material are dramatically changed. Scaling is allowable in case if the designer manages to avoid falling into the area of a strong dispersion near the resonance.

Effective electric and magnetic properties of a three-dimensional collection of nonmagnetic polaritonic spheres have been investigated in [27]. Structure based on a periodic crystal wherein the respective polaritonic spheres are arranged on two interpenetrating simple cubic lattices, has been discussed in [28]. An example comprising $LiTaO_3$ and n-type Ge

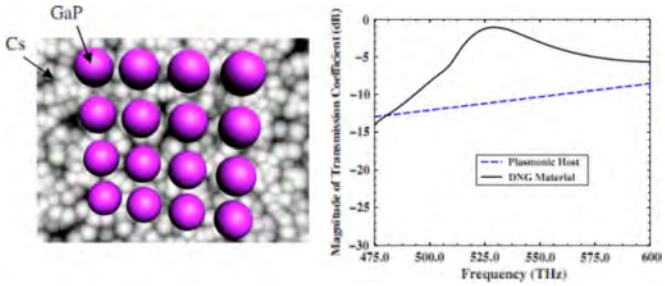

Fig. 6. DNG optical metamaterial constructed from nanostructured dielectric spheres, operating in magnetic mode, embedded in negative permittivity host [27]. (a) Geometry.(b) Transmission coefficient.

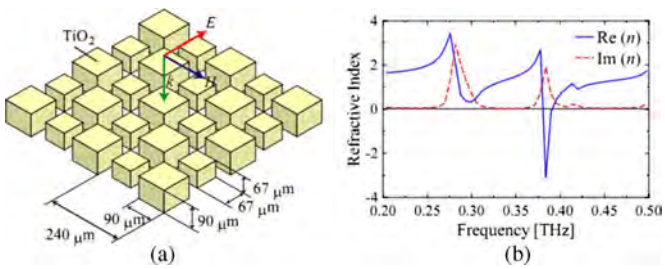

Fig. 7. (a) Configuration to achieve the negative refractive index. (b) Spectrum of the refractive index in this configuration [20].

spheres revealed a negative refractive index centered around $\lambda_c \approx 12.238$ μm. By using other available polaritonic materials, the center wavelength λ_c of the negative refractive index band can be correspondingly tuned over a wide frequency range.

Isotropic all-dielectric metamaterial at optical frequency has been theoretically investigated in [29]. In this paper, the periodic array of GaP spheres implanted inside cesium Cs host material with a measured plasma wavelength $\lambda_p = 0.41$ μm was considered [see Fig. 6(a)]. Transmission coefficient of the composite structure is shown in Fig. 6(b). The spheres operate at their magnetic resonant mode and can provide negative effective permeability. A combination of this with the negative permittivity of cesium below its plasma resonance offers DNG behavior. In comparison to the double-sphere resonators design, only one set of resonators is involved and a wider bandwidth can be expected.

As compared with spherical resonators, cubical dielectric resonators are easy to fabricate. The natural method to shift operating dielectric metamaterial frequencies to the THz spectrum region is to scale dielectric resonators size to micrometers. Terahertz metamaterials based on the Mie resonance of polycrystalline TiO_2 cube arrays on Al_2O_3 substrate [see Fig. 7(a)] were experimentally demonstrated in [20]. The resonant responses occur at the frequency around 0.28 THz, where wavelengths almost ten times larger than the periodicity of the sample. Adjusting sizes of two sets of cubes with different dimensions makes it possible to match resonance frequencies with negative permittivity and permeability. Simulation results [see Fig. 7(b)] shows the negative refraction is observed at frequency around 0.38 THz.

The magnetic activity based on Mie resonance can also be achieved within a broad frequency range from the terahertz to the deep infrared region by suitable choice of materials and

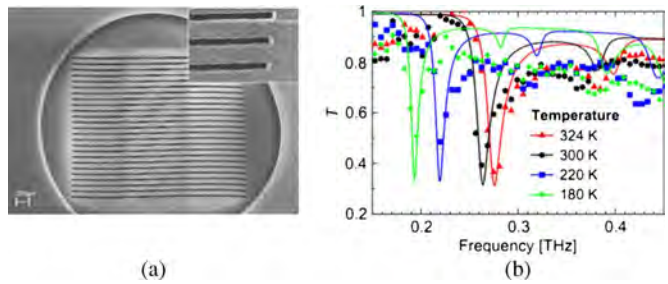

Fig. 8. (a) Scanning electron microscope picture of one of the samples. (b): Examples of amplitude transmittance spectra. A shift of the magnetic resonance from 0.287 THz to 0.204 THz with temperature is clearly visible. Points: measured values, lines: spectra calculated using the transfer matrix [32].

particle dimensions, for example, polaritonic crystal $(LiTaO_3)$ have a permittivity of 400 at approximate 3.5 THz [27]. Moreover, the BST dielectric composites can be expected to possess electrically tunable properties, which may increase the range of potential applications [30], [31].

C. Tunability of Dielectric THz Metamaterial

The metamaterial described in [32] consist of arrays of high permittivity rectangular rods made of strontium titanate $SrTiO_3$ (STO) by femtosecond laser micromachining. Wafers of STO with a thickness of 20–50 μm were perforated by a focused laser beam in the shape of parallel lines, thus creating rods with a width of several tens of microns and a periodicity of less than 100 μm [see Fig. 8(a)]. For incident electric field polarized perpendicular to the rods, the arrays exhibit a series of Mie resonances accompanied by an effective magnetic response [33]. It appears that the lowest-order resonances are sufficiently strong to induce a response described by a negative effective permeability.

Transmittance spectra of the samples measured using time-domain terahertz spectroscopy are shown in Fig. 8(b). The amplitude transmittance exhibits a clear dip, which corresponds to the lowest Mie resonance. Upon cooling, the permittivity of STO increases due to phonon mode softening; therefore, the resonant frequency decreases. The magnetic permeability retrieved from the measured transmission spectra revealed the negative value of the permeability in the narrow frequency range between 0.23–0.24 THz.

Dielectric cylinders can be effectively used for **cloaking in THz spectrum** [34]. Mie theory was applied to high-ε micrometer-sized BST cylinders and results showed that the ferroelectric rods exhibited a strong magnetic resonance dependent on the cylinder radii. The rods magnetic plasma frequency was engineered such that the cloak shell displays a piece-wise variation in the radial component of the permeability. Results clearly show that cloaking of any wavelength scaled object located at the interior is achieved at 0.58 THz for the present device. Additionally, a relatively high transmissivity level was obtained. These results show the potential of this all-dielectric solution for cloaking applications at microwave and terahertz frequencies.

D. Ferroelectrics and Ferromagnetics Based MTM

The dielectric properties of **ferroelectric** materials can be tuned both by external dc (low-frequency) electric field and by

temperature up to the THz range. Ferroelectric materials are especially attractive for tunable applications owing to the potentially low production cost and a high integrability.

Currently the displacement type ferroelectrics are most popular as tunable materials for microwave applications. The typical representative of displacement type ferroelectrics is solid solution $Ba_xSr_{1-x}TiO_3$ (BST). This material demonstrates dielectric nonlinearity up to 2 THz at room temperature [35]–[37]. The incipient ferroelectric $SrTiO_3$ (STO) also can be used for THz MTM design. It was experimentally demonstrated up to 11% variation of the $SrTiO_3$ (STO) film permittivity induced by an applied voltage 150 V (100 kV/cm) at room temperature [35]. No dielectric dispersion is observed between 1 MHz and 0.5 THz. The average dielectric constant was about 350 and substantially decreases with frequency at frequency higher than 1 THz [35].

The tunability of ferroelectrics is defined as a variation of the dielectric permittivity under the applied electric field. The tunability of STO can be improved by using strained multilayer structures [36], [37]. For example, the multilayer structures composed of the $SrTiO_3$ and $DyScO_3$ (DSO) thin layers deposited on DSO substrate demonstrate up to 65% variation of the permittivity and up to 33% modulation of the power transmission of THz waves at 500 GHz and under 100 V (67 kV/cm) biasing voltage [36] at room temperature. The multilayer consists of four STO/DSO bilayers with 50 nm of the thickness of each layer, i.e., the total thickness of STO was 200 nm). The average value of the dielectric constant of such multilayer structures is about 1000–1500 at room temperature and zero biasing field. Strained samples show a significant enhancement of the tunability of both the permittivity and the loss factor. The multilayer samples show a potential applications as THz modulators: a power modulation of up to 40% near 1 THz revealed the multilayer sample composed of four STO separated by three DSO 50-nm thick layers [37].

Dielectric characteristics of ferroelectric materials are strongly dependent on temperature. It was experimentally observed that for strained multilayer sample consisting of four STO/DSO bilayers (of 50 nm each) deposited on a DSO single-crystal substrate 1.5 times decreasing temperature leads to 2 times decreasing the dielectric permittivity at 0.5 THz [36].

The analysis of dielectric constant frequency dependence of STO thin film (650 nm STO film on MgO substrate with orientation [100]) measured at various temperatures [38] makes it possible to conclude that there is no frequency dispersion of the permittivity up to 0.7 THz at temperatures higher than 200 K. For such films the increase of the temperature from 23 up to 290 K provides the dielectric constant reducing from 400 to 200. The highest temperature nonlinearity of dielectric constant was observed at temperatures below 160 K. At the same time, decreasing of the temperature leads to catastrophic increase of loss factor [38]. The loss factor of thin STO film at 23 K and 0.5 THz is about unity [38]. At 290 K and 0.5 THz for STO thin film $\tan\delta \cong 0.08$ [38], and for STO ceramics $\tan\delta \cong 0.06$ [39].

In this way, the electrical tunability of dielectric permittivity of strained multilayer structures based on displacement type ferroelectrics can reach 65% at THz frequency. The temperature tunability is higher than 70%.

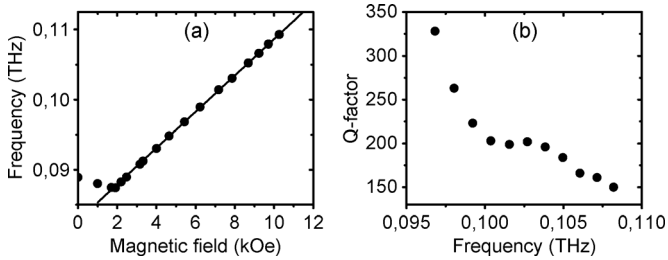

Fig. 9. (a) Resonant frequency of the $BaAl_2Fe_{10}O_{19}$ resonator as a function of the external magnetic field. (b) Loaded Q-factor of the resonator [50].

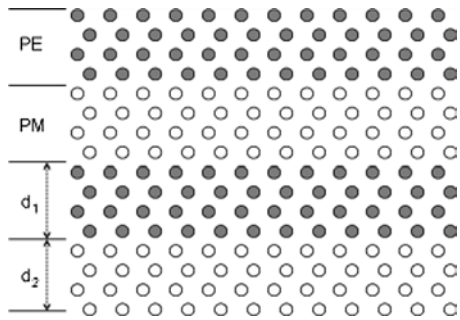

Fig. 10. Schematic of the oxide superlattice potentially showing negative refraction [51].

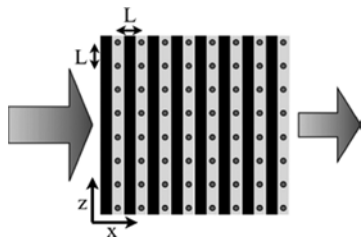

Fig. 11. Structure of the ferrite (black) and dielectric (gray) composite configuration with a square wire grid (black circles) [52].

Different ferroelectrics based MTM are worth to mention:

— The subwavelength metallic structures based on SRR loaded by ferroelectric capacitors or SRR array formed on uniform ferroelectric film [40]–[42]. SRR can be described by an L-C equivalent circuit and thus the resonance frequency can be tuned by the capacitance value, which is a function of ferroelectrics dielectric permittivity and therefore can be tuned by electric field and temperature.

— Isotropic composites based on Mie resonance of the ferroelectric medium [32], [43]–[45]. Measurements and simulations showed that the dielectric material composed of BST-MgO dielectric particles exhibited a strong sub-wavelength magnetic resonance at the first Mie resonance and possessed isotropic negative permeability resulted from the displacement current excited in the particle. The dielectric particle is equivalent to a magnetic dipole at the magnetic resonance adjusted by the size and permittivity of the particles.

Other materials that could be used for metamaterial design are **ferromagnetics**. The ferromagnetic based MTM operate in vicinity of ferromagnetic resonance (FMR). In order to observe the resonance in the THz frequency range, one needs to apply a

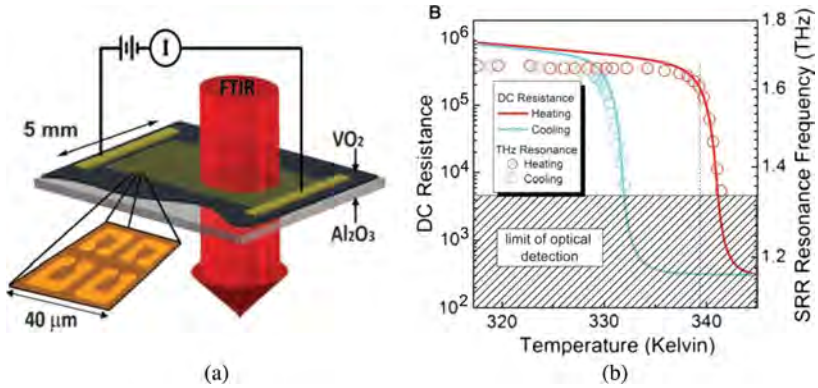

Fig. 12. (a) Memory-oxide hybrid-metamaterial device consists of a gold SRR array on a VO_2 film. It is mounted on a temperature control stage with attached electrodes. (b) Simultaneous dc-transport and far-infrared probing of the metamaterial measurement on its insulator-metal transition [67].

large external magnetic field or to use a ferromagnetic material with a large magnetocrystalline anisotropy field H_A. Such materials with a large H_A are hexagonal ferrites.

Magnetic and dielectric resonances in the sub-terahertz (sub-THz) frequency range are observed in pure and Al-substituted hexagonal barium ferrite. Sub-THz resonances in hexaferrites reveal the potential for tunable ferrite-based devices, which are commonly used as frequency selective elements in radars, telecommunication, and measurement systems [46]–[52]. The substitution of iron (Fe) in Ba-hexaferrite by aluminum (Al) significantly increases the magnetization anisotropy so that FMR frequency $f_{\rm FMR}$ can be easily obtained in subterahertz range for reasonable values of bias magnetic fields H [50]–[52].

Magnetic excitations in a single-crystal hexagonal ferrite $BaAl_2Fe_{10}O_{19}$ are observed in the frequency range of 0.09–0.11 THz for nominal external bias fields [see Fig. 9(a)]. It is clear that linear increase in $f_{\rm FMR}$ versus H implies FMR around 0.5 THz for $H = 150$ kOe. Moreover, one may use thin hexagonal ferrite films in which surface spin pinning increases significantly spin-wave resonance frequencies up to unity of terahertz. Note, that Q-factor of the resonators is remarkably high [see Fig. 9(b)]. It implies potential use of the ferrite for terahertz signal processing.

Composite materials composed of ferrite and piezoelectric or ferroelectrics are promising for application. One of the distinguishing features of the devices based on composite materials is the possibility of simultaneous electric and magnetic tuning (dual tuning) of their performance. In particular, resonators, phase shifters, delay lines, and filters based on the layered structures have been demonstrated [53]–[61]. Terahertz ferrite-piezoelectric composite materials were suggested in [51]. A magnetoelectric coupling in the ferrite-piezoelectric bilayers has been experimentally demonstrated at sub-terahertz frequencies.

A possible realization of ferrite-piezoelectric or ferrite-ferroelectric layered structure is shown in Fig. 10. It consists of piezoelectric (PE) and piezomagnetic (PM) oxide material layers. Complex ferroelectric (FE), PE, and PM oxide materials are well known for their extraordinary responses to optical and THz frequencies.

Another composite structure using ferrites is shown in Fig. 11. This composite consists of BaM ferrite lamina (black)

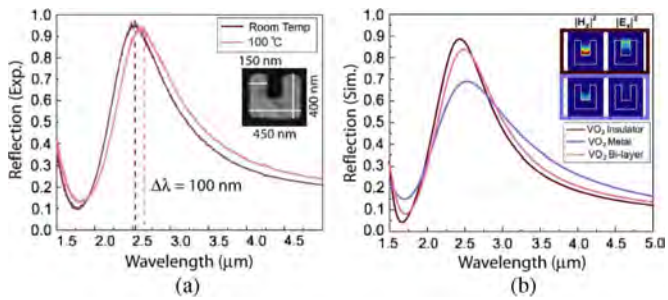

Fig. 13. Active hybrid-SRR arrays [68]. (a) Near-IR reflection spectra of self-aligned 150 nm Ag/60 nm VO_2 hybrid-SRR arrays. The magnetic resonance shifts by 100 nm after the VO_2 heating. (b) FDTD simulation data.

with in-plane anisotropy providing a low loss negative μ, dielectric slabs (gray), and a monodirectional square wire grid centered in the dielectric (black circles) providing the negativeε.

Thus, artificial composite materials (or metamaterials) in the form of hexaferrite-piezoelectric or hexaferrite-ferroelectric structures have a great potential application for THz science and technology. In particular, they could be used for development of dual electric and magnetic field tunable resonators, filters, and phase shifters operating at THz frequencies.

E. MTM Based on Phase Change Materials

Tunable metamaterials can be realized by the material crystalline phase change, which leads to the change of dielectric properties. The crystalline phase transition leads to electrical and optical property changes such as resistivity, color, and refractive indices. Currently, metamaterial research based on phase change materials (PCM) can be found from materials with metal-to-insulator transition such as vanadium oxide and from color changing chalcogenide glasses. They show optical property changes not only in THz spectrum range but also in NIR range.

Basic idea of PCM based tunable metamaterials is to pattern the PCM with periodic structures leading to photonic response change by phase control with thermal, optical, and electrical stimuli. Crystalline morphology change requires temperature increase and cool-down process, so that the thermal stimulus is more fundamental control than optical and electrical ones.

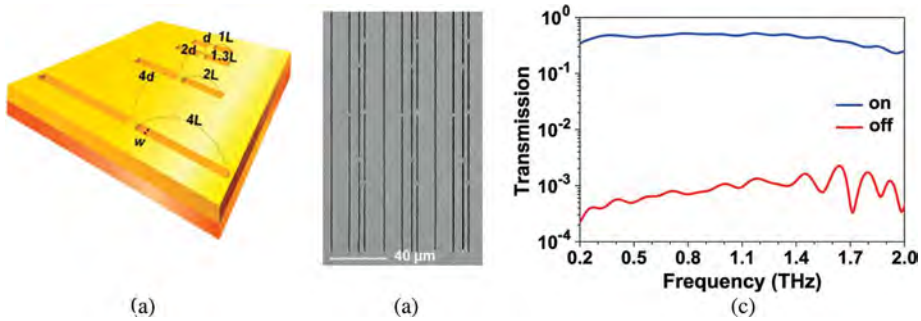

Fig. 14. Broad-band active metamaterial in the THz region [70]. (a) Schematics for resonator patterns on a VO_2 thin film, (b) SEM image. (c) Transmission of the broad-band resonator for 305 K (blue) and 375 K (red).

VO_2 based metamaterials are promising for a design of functional MTM for THz applications. VO_2 is a correlated electron material that exhibits an insulator-metal phase transition (IMT) that can be thermally [62], electrically [63], [64], or optically [65] controlled. The transition is highly hysteretic and has been previously shown to exhibit memory effect [66]. The phase transition also affects the dielectric properties of VO_2 in a specific way, changing the dielectric permittivity. The IMT characteristic of VO_2 is useful to metamaterials with memory effect, tunable and active metamaterials.

An example of memory device [67] is illustrated by use of a single-layer gold SRR array patterned on a 90 nm-thin film of VO_2 (Fig. 12(a)). The hysteresis associated with the VO_2 can be observed by measuring the dc resistance of the sample (Fig d.2, solid lines). The phase transition also affects the dielectric properties of VO_2 making change of the capacitance and metamaterial resonance frequency during IMT process (Fig d.2, circle). $T = 338.6$ K was chosen for maximizing the memory effect (Fig. 12(b), dashed line). The excitation voltage pulse was applied using the electrical lead for local heating $\geq T_\alpha = 0.11$ K causing an increase in the capacitance. Once the voltage pulse stops, the VO_2 quickly ($\leq$25 ms) thermalizes back to the bias temperature of 338.6 K. The device is suitable for hybrid-metamaterial design to obtain memory effect.

VO_2 also can be applied to the frequency tunable metamaterial [68]. FTIR reflection data and FDTD simulation show the red shifted resonance peak position as the VO_2 temperature increases (Fig. 13).

Ultra-broad-band metamaterial thin film with 0.2 $\sim$ 2 THz range is presented in [69], [70]. The rectangular structures with micro- and nano-patterned dimensions on VO_2 film show well-defined resonance. With metal phase of VO_2 film, the transmission amplitude decreases, especially on nano-patterned structure. Combining this single nano-patterned antenna with various resonances (called multi-antennas) per unit cell shows active broad-band antenna in THz region of on/off ratio about 10^3 (Fig. 14).

Chalcogenide glass based active metamaterials have been also of interest due to potential applications in next generation memory materials [71]. When the pulse light of picojoules is incident to the chalcogenide glass in nanoscale region, electrical, thermal, and mechanical properties of the glass are changed reversibly including the optical property like refractive index. These properties are also very profitable switching and modulation of metamaterials [72].

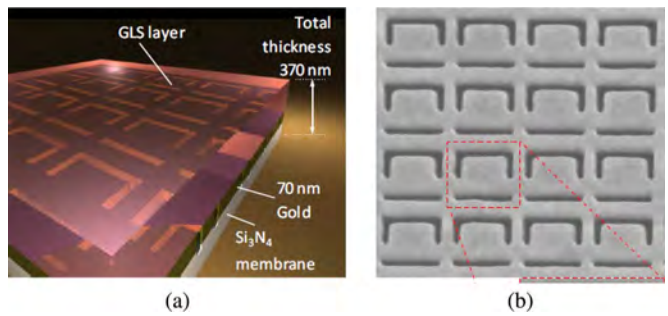

Fig. 15. Schematic picture of active metamaterial composed of GLS layer and a planar gold metal layer on a silicon nitride membrane [77]. (b) Scanning electron microscope image of the asymmetric split-ring (ASR) slit array metamaterial before GLS deposition.

In 2010, active metamaterials with chalcogenide glass of gallium lanthanum sulfide (GLS) have been studied for the first time [73], [74]. Germanium antimony telluride (GST) has been famous with a major chalcogenide material, and widely investigated by far. Unfortunately, GST has high absorption coefficient from the visible to mid-IR range. On the other hand, GLS is transparent from 500 nm to $\sim$ 10 μm [75]. In [73], [74], about a 150 nm shift of a Fano-resonance mode was observed in near-IR range using metamaterials based on an array of asymmetrically split ring resonator (ASR) [76], [77]. GLS thin film with 200 nm thickness is sandwiched between molybdenum electrodes (Fig. 15) supplying maximum 20 V at the frequency of 3 Hz. During excitation, GLS phase is changed from amorphous to crystalline and vice versa, and also absorption, reflection, and transmission spectrum of metamaterials are shifted by about 150 nm due to the change of refractive index of GLS. The transition time of switching in this case is reported by the order of 50 $\sim$ 100 ns.

F. Layered Metal-Dielectric Structures of MTM

Metal-dielectric composite structures can also be used to form metamaterials for THz. In [78] the layered metal-dielectric structure with periodic array of cross-dipole apertures has the needed property to be the perfect lens in THz range.

The photolithography technique was used for a fabrication of a square array of cross-dipole holes. A schematic of one unit cell and the incident polarization are shown in Fig. 16(a).

As shown in Fig. 16(b), the measured results clearly show two transmittance bands in mid-IR frequencies. The high-fre-

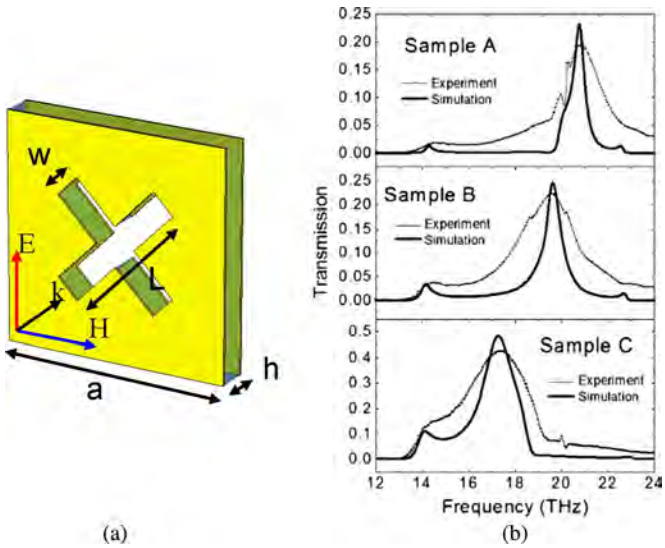

Fig. 16. (a) Scheme of one unit cell of the configuration and (b) simulated (solid) and measured (dotted) transmission spectra of samples A, B, and C with different arm length L [78].

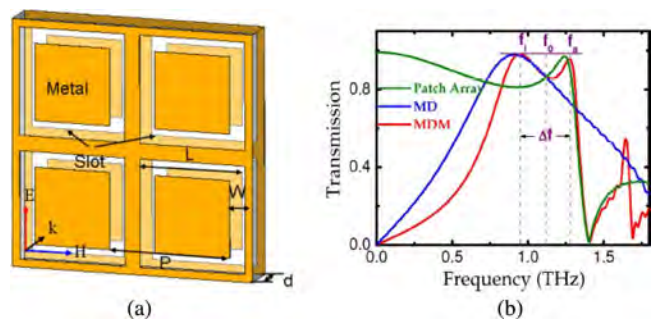

Fig. 17. (a) Schematic of a square array of square-loop-shaped slots with normal incident electromagnetic field and (b) comparison of the transmission spectra of the chosen MDM with the MD structure of only one single metallic layer, as well as the sandwich patch array [79].

quency transmission peak is the guided mode associated with the surface plasmon polariton (SPP), and its location strongly depends on the arm length of the cross-dipole. The lower-frequency transmission peak is proposed to be the antisymmetric plasmon polariton mode, and its location hardly shifts as the size of the cross-dipole varies.

The metal–dielectric–metal (MDM) sandwich plasmonic structure presented in [79] has the broad pass-band resonant transmission response at THz frequencies. The structure consists of periodic square-loop slotted metallic arrays on both sides of a thin dielectric substrate [see Fig. 17(a)]. MDM structure of double metallic layers has a much flatter transmission top [see Fig. 17(b)] in comparison with the structure with only one single metallic layer of the same square-loop hole array. Clearly, the additional second array leads to an ultrawide passband. The resonance top in the MDM structure is pulled broadly by the two resonance frequencies $\mathrm{f_i} = 0.95$ THz and $\mathrm{f_a} = 1.28$ THz away from each other, and the simulated passband response centers at $\mathrm{f_0} = 1.12$ THz.

For such a MDM filter design, the permittivity ε_d, the thickness d of the substrate dielectric, and the main geometry parameters of the slot naturally influence the frequency response. The

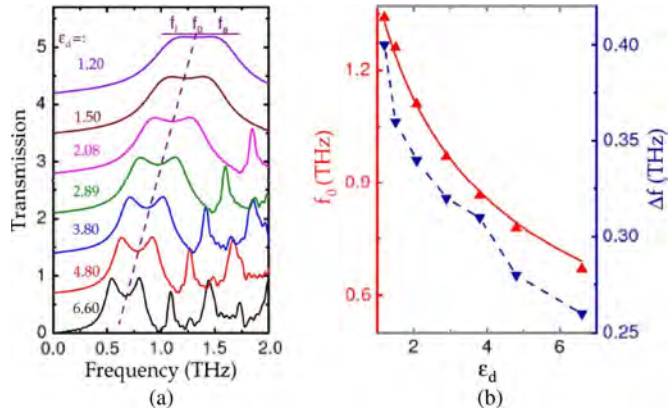

Fig. 18. (a) Computed transmission spectra for various permittivity ε_d of the middle dielectric substrate. (b) Dependence of the simulated values of the center resonance frequency $\mathrm{f_0}$ with corresponding $\Delta\mathrm{f}$ on ε_d [79].

transmission of the MDM structure with different permittivity ε_d of the dielectric is plotted in Fig. 18. Decreasing the permittivity ε_d, $\mathrm{f_0}$ is blueshifted and $\Delta\mathrm{f}$ is broadened.

Potential applications of the structure can be found in THz tunable filters. One can control the parameters of MTM implemented in the layered metal-dielectric structure using materials with tuned permittivity, for example liquid crystals or ferroelectrics.

G. Liquid Crystal Based MTM Structures

Liquid crystals (LC) have anisotropic optical, electrical, and magnetic properties that are sensitive to external fields [80]. Furthermore, they are also compatible with almost all widely used optoelectronic materials and possess very broadband (near UV to infrared) transparency with large optical birefringence n [81]. Recent studies indicate that LCs can also be used for microwave tuning applications [82], [83]. Their fluid nature allows easy incorporation into various geometries and nanometer scale pore sizes [81].

Bulk metamaterials, which consist of a LC host and coated dielectric (non-magnetic) spheres randomly distributed throughout a LC host, are suggested in [84], [85] (Fig. 19).

The effective permittivity ε_eff and permeability μ_eff of bulk material was computed by using the Maxwell Garnet mixing theory. In [84] an operating frequency around 3.8 THz is chosen. The parameter of the coated sphere is radius $\mathrm{r_2} = 4.15$ μm and the core radius $\mathrm{r_1} = 4$ μm. One can clearly see from characteristics in Fig. 19(c) that when the relative permittivity of the LC is changed from 2 to 3 to 4, the corresponding index of refraction n_eff changes from -1 to 0 and to about $+1$. In other words, the MTM can be tuned to have a negative index of refraction, a zero index of refraction, or a positive index of refraction for the same operating frequency by controlling an electric field or a magnetic field. The Drude material spheres with no coating dispersed in a LC host are presented in [85].

A two-dimensional periodic metamaterial structure with reconfigurable negative-zero-positive index of refraction is shown in Fig. 20 [86]. The structure is infinite in the $\pm y$-direction and periodic with period p in the $\pm x$-direction. A magnetic resonator comprises thin layer of alumina of thickness d. The two

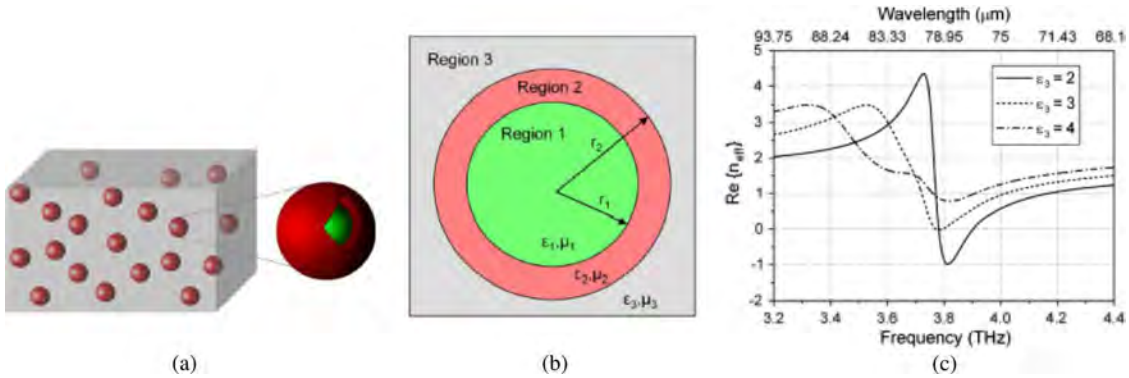

Fig. 19. (a) Overall structure of 3-D metamaterial formed by randomly dispersing spherical core-shell molecules in a LC host; (b) cross section of a single coated sphere molecule. (c) Real part of refractive index n_{eff} versus frequency for three different values of ε_3 [85].

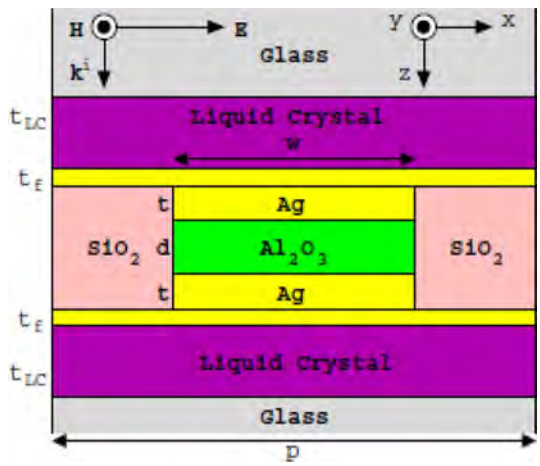

Fig. 20. A two-dimensional metamaterial with thick liquid crystal superstrate and substrate layers having a reconfigurable index of refraction [86].

strips of silver of width w and thickness t separated by a negative permittivity needed for negative-index behavior is provided by thin silver films of thickness t_f bounding the periodic array of magnetic resonators from the $\pm z$-directions. Finally, the space between neighboring magnetic resonators is filled with silica. A layer of LC with thickness t_{LC} is used both as the superstrate and the substrate. A monochromatic wave with the electric field polarized in the x-direction is assumed to illuminate the structure at normal incidence propagating in the $+z$-direction.

The effective refraction coefficient n changes with changing of ε_{LC} in the range $2 \geq \varepsilon_{LC} \geq 3$. With $\varepsilon_{LC} = 2$, the MTM exhibits a negative index band between 1.37 μm and 1.47 μm. The proposed near-IR MTM possesses a reconfigurable index of refraction over a negative-zero-positive range from $\lambda = 1.37$ μm to $\lambda = 1.47$ μm, which represents a 7.1% fractional bandwidth.

A rather similar structure was presented in [87]. It was considered a trilayer MDM structure patterned with a two-dimensional square lattice of rectangular holes through all three layers infiltrated by LC (Fig. 21). Even a small amount of LC reveals a substantial tunability of such structures, including reversal of the sign of the refractive index. This is achieved by employing the reorientation of the LC director using an external field, as well as by implementing the temperature dependence of the LC refractive index.

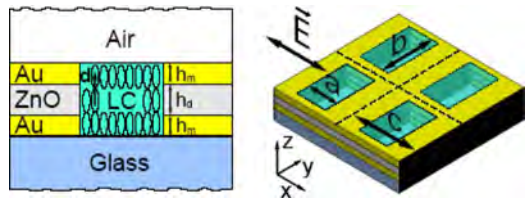

Fig. 21. Trilayer fishnet metamaterial on a glass substrate. Left: Schematic of the layers. Right: Four unit cells of the structure [87]. h_m is the thickness of metal (Au), h_d is the thickness of dielectric (ZnO). Both substrate and cladding are semi-infinite. Light is polarized along x axis.

III. Conclusion

Design of tunable THz metamaterials is a challenging task. As shown before, variety of different ways to design THz MTM tunable structures play special roles. Since conventional THz optic devices usually do not have a possibility to change their properties, THz tunable MTM look extremely attractive for manipulating electromagnetic waves in THz spectrum. The overview of results obtained recently confirms that there are some promising directions of active THz metamaterial design [88].

Different ways to perform tuning can be applied to MTM structures: temperature control, optical control, electric or magnetic field control. Temperature control is suitable for changing dielectric or conducting properties within the MTM structure. In case of an active dielectric (ferroelectrics) using a control of the dielectric permittivity is available. It is a natural way of changing ferroelectric permittivity by temperature variation. Unfortunately this method is rather slow. At the same time, the dielectric permittivity of ferroelectrics can be also changed by voltage control, though the electric field is rather high: 50–100 V/μm.

Control by light illumination is one of the most interesting ways to perform tuning of artificial structure parameters. It is the fastest way of control and besides it allows getting more precise uniform value of the controlling impact in comparison with the temperature control. The magnetic field control demands to use ferromagnetic material and the magnetic fields of a moderate level: 5–10 kOe. The combination of ferroelectric and ferromagnetic materials looks very promising for tunable MTM design. The MTM structure can be designed using LC as a host material. The sensitivity of LC material to external fields can be

used for designing tunable devices and materials. Nematic LCs suit very well for this purpose.

Among different MTM designs introduced to operate in THz range the most popular are MTM utilizing SRR or/and wire medium. SRR-based MTM are well investigated and there are no fundamental difficulties for manufacturing. They can have different shapes providing different transmission coefficient behavior. The SRR can be placed on a flexible substrate that leads to many practical applications. The control of operating spectrum of SRR MTM is based on the tunability of the gap parameters, which leads to the changes in conductivity or capacitance. Temperature and voltage control as well as optical control can be effectively used for manipulating the SRR array electromagnetic characteristics. Important drawback of SRR or/and wire medium MTM is a rather high loss level due to the conducting parts of the MTM while the frequency is increasing.

MTM based on dielectric resonators are deprived of conductive losses what is especially important for the THz frequencies. Dielectric resonators can have spherical, cylindrical or cubic shape. A regular array of these resonators can form isotropic 3D MTM for THz range. From a loss reduction and fabrication tolerance point of view, dielectric resonators are promising candidates for manufacturing THz metamaterial structures. Dielectric resonators based MTM provides higher isotropy and homogeneity in comparison with SRR and wire medium based MTM. It is easier to fabricate bulk 3D metamaterials using dielectric resonators. Chemical synthesis based on self-assembly is a promising method to perform 3D bulk metamaterials with periodically assembled micrometer-sized resonant inclusions [89]. The most promising tuning technology is manipulating dielectric properties of the host matrix of the all dielectric metamaterials or the dielectric resonators itself. In this case electric field controllable liquid crystal or ferroelectric material can be effectively used as a host matrix.

Most importantly, continuing development of micro- and nano-technology for ingenious MTM structures gives hope for success in engineered design of tunable MTM for THz applications. The assessment of MTM technologies from the practical point of view is a very important issue. That is why we believe that the reader of this review paper is able to choose a suitable material and appropriate technology on the base of his own criteria.

REFERENCES

[1] W. L. Chan, J. Deibel, and D. M. Mittleman, "Imaging with terahertz radiation," *Rep. Progr. in Phys.*, vol. 70, no. 8, pp. 1325–1379, 2007.

[2] P. de Maagt, "Terahertz technology for space and earth applications," in *First Eur. Conf. on Antennas Propag.*, Nov. 6–10, 2006, pp. 1–4.

[3] S. J. Pendry, "Metamaterials and the control of electromagnetic fields," in *OSA Tech. Dig. Conf. Coherence and Quantum Opt.*, 2007 [Online]. Available: CD-ROM, paper CMB2

[4] D. Schurig *et al.*, "Metamaterial electromagnetic cloak at microwave frequencies," *Science*, vol. 314, pp. 977–980, 2006.

[5] J. B. Pendry, A. J. Holden, D. J. Robbins, and W. J. Stewart, "Magnetism from conductors and enhanced nonlinear phenomena," *IEEE Trans. Microw. Theory Techn.*, vol. 47, pp. 2075–2084, 1999.

[6] D. R. Smith, W. J. Padilla, D. C. Vier, S. C. Nemat-Nasser, and S. Schultz, "Composite medium with simultaneously negative permeability and permittivity," *Phys. Rev. Lett.*, vol. 84, pp. 4184–4187, 2000, 3.

[7] H. Tao, N. I. Landy, K. Fan, A. C. Strikwerda, W. J. Padilla, R. D. Averitt, and X. Zhang, "Flexible terahertz metamaterials: Towards a terahertz metamaterial invisible cloak," in *IEEE Int.Electron Devices Meeting '2008*, San Francisco, CA, Dec. 15–17, 2008, pp. 1–4.

[8] A. K. Azad, H.-T. Chen, X. Lu, J. Gu, N. R. Weisse-Bernstein, E. Akhadov, A. J. Taylor, W. Zhang, and J. F. O'Hara, "Flexible quasi-three-dimensional terahertz electric metamaterials," *THz Sci. Technol.*, vol. 2, no. 1, pp. 15–22, 2009.

[9] H. Tao, C. M. Bingham, D. Pilon, K. Fan, A. C. Strikwerda, D. Shrekenhamer, W. J. Padilla, X. Zhang, and R. D. Averitt, "A dual band terahertz metamaterial absorber," *J. Phys. D: Appl. Phys.*, vol. 43, p. 225102, 2010.

[10] F. Miyamaru, M. Wada Takeda, and K. Taima, "Characterization of terahertz metamaterials fabricated on flexible plastic films toward fabrication of bulk metamaterials in terahertz region," *Appl. Phys. Express*, vol. 2, no. 4, p. 042001, 2009.

[11] H. Tao, A. Strikwerda, C. Bingham, W. J. Padilla, X. Zhang, and R. D. Averitt, "Dynamical control of terahertz metamaterial resonance response using bimaterial cantilevers," in *PIERS Proc.*, Cambridge, USA, Jul. 2–6, 2008, pp. 870–873.

[12] H. Tao, A. C. Strikwerda, K. Fan, W. J. Padilla, X. Zhang, and R. D. Averitt, "MEMS based structurally tunable metamaterials at terahertz frequencies," *J. Infrared, Millim. THz Waves*, no. 32, pp. 580–595, 2011.

[13] W. M. Zhu, H. Cai, T. Mei, T. Bourouina, J. F. Tao, G. Q. Lo, D. L. Kwong, and A. Q. Liu, "A MEMS tunable metamaterial filter," in *Proc. IEEE 23rd Int. Conf. on Micro Electro Mech. Syst. (MEMS), '2010*, Wanchai, Hong Kong, Jan. 24–28, 2010, pp. 196–199.

[14] J. Han and A. Lakhtakia, "Semiconductor split-ring resonators for thermally tunable terahertz metamaterials," *J. Modern Opt.*, vol. 56, pp. 554–557, 2009.

[15] N.-H. Shen, M. Kafesaki, T. Koschny, L. Zhang, E. N. Economou, and C. M. Soukoulis, "Broadband blueshift tunable metamaterials and dual-band switches," *Phys. Rev. B*, vol. 79, p. 161102, 2009.

[16] H.-T. Chen, W. J. Padilla, R. D. Averitt, A. C. Gossard, C. Highstrete, M. Lee, J. F. O'Hara, and A. J. Taylor, "Electromagnetic metamaterials for terahertz applications," *Terahertz Science and Technology*, vol. 1, no. 1, pp. 42–50, 2008.

[17] H. Chen, W. J. Padilla, R. D. Averitt, J. F. O'Hara, and M. Lee, "Active Terahertz Metamaterial Devices," U.S. Patent 7826504, Nov. 2, 2010.

[18] Q. Zhao, J. Zhou, F. Zhang, and D. Lippens, "Mie resonance based dielectric metamaterial," *Materials Today*, vol. 12, pp. 60–69, 2009.

[19] M. S. Wheeler, J. S. Aitchison, and M. Mojahedi, "Three-dimensional array of dielectric spheres with an isotropic negative permeability at infrared frequencies," *Phys. Rev. B*, vol. 72, p. 193103, 2005.

[20] K. Shibuya *et al.*, "Terahertz metamaterials composed of TiO2 cube arrays," in *Proc. 2nd Int. Congress on Advanced Electromagnetic Mater. in Microw. and Opt.*, Pamplona, Spain, Sep. 21–26, 2008, pp. 777–779.

[21] T. Lepetit, E. Akmansoy, M. Pate, and J.-P. Ganne, "Experimental measurement of negative index in an all-dielectric metamaterial," *Appl. Phys. Lett.*, vol. 95, no. 12, pp. 121101–121101-3, 2009.

[22] X. Cai, R. Zhu, and G. H. , "Experimental study for metamaterials based on dielectric resonators and wire frame," *Metamater.*, vol. 2, no. 4, pp. 220–226, Dec. 2008.

[23] Y. G. Ma, L. Zhao, P. Wang, and C. K. Ong, "Fabrication of negative index materials using dielectric and metallic composite route," *Appl. Phys. Lett.*, vol. 93, no. 18, p. 184103, 2008.

[24] O. G. Vendik and M. S. Gashinova, "Artificial double negative (DNG) media composed by two different dielectric sphere lattices embedded in a dielectric matrix," in *Proc. 34th Eur. Microw. Conf. 2004*, Oct. 2004, pp. 1209–1212.

[25] I. Vendik, M. Odit, and D. Kozlov, "3D isotropic metamaterial based on a regular array of resonant dielectric spherical inclusions," *Metamater.*, vol. 3, no. 3–4, pp. 140–147, 2009.

[26] I. Vendik, M. Odit, and D. Kozlov, "3D metamaterial based on a regular array of resonant dielectric inclusions," in *Radioengineering, Proc. Czech and Slovak Tech. Univ. and URSI Commities*, Jun. 2009, vol. 18, no. 2, pp. 111–116.

[27] K. C. Huang, M. L. Povinelli, and J. D. Joannopoulos, "Negative effective permeability in polaritonic photonic crystals," *Appl. Phys. Lett.*, vol. 85, p. 543, 2004.

[28] V. Yannopapas and A. Moroz, "Negative refractive index metamaterials from inherently non-magnetic materials for deep infrared to terahertz frequency ranges," *J. Phys.: Condensed Matter*, vol. 17, no. 25, pp. 3717–3734, 2005.

[29] B. J. Seo, T. Ueda, T. Itoh, and H. Fetterman, "Isotropic left handed material at optical frequency with dielectric spheres embedded in negative permittivity medium," *Appl. Phys. Lett.*, vol. 88, p. 161122, 2006.

[30] G. Vélu *et al.*, "Electrical characterizations of paraelectric BST thin films up to 1 THz," *Ferroelectrics*, vol. 353, p. 29, 2007.

[31] B. Hou, G. Xu, H. Wong, and W. Wen, "Tuning of photonic bandgaps by a field-induced structural change of fractal metamaterials," *Opt. Express*, vol. 13, p. 9149, 2005.

[32] H. Němec *et al.*, "Tunable terahertz metamaterials with negative permeability," *Phys. Rev. B*, vol. 79, p. 241108(R), 2009.

[33] S. O'Brien and J. B. Pendry, "Photonic band gap effects and magnetic activity in dielectric composites," *J. Phys.: Condensed Matter*, vol. 14, p. 4035, 2002.

[34] D. P. Gaillot, C. Croënne, and D. Lippens, "An all-dielectric route for terahertz cloaking," *Opt. Express*, vol. 16, no. 6, pp. 3986–3992, 2008.

[35] P. Kužel, F. Kadlec, H. Němec, R. Ott, E. Hollmann, and N. Klein, "Dielectric tunability of SrTiO3 thin films in the terahertz range," *APL*, vol. 88, p. 102901, 2006.

[36] P. Kužel, F. Kadlec, J. Petzelt, J. Schubert, and G. Panaitov, "Highly tunable $SrTiO_3/DyScO_3$ heterostructures for applications in the terahertz range," *APL*, vol. 91, p. 232911, 2007.

[37] F. Kadlec, C. Kadlec, J. Schubert, G. I. Panaitov, and P. Kužel, "Modulators of THz radiation based on SrTiO3 epitaxial thin films," in *33rd Int. Conf. on Infrared, Millim. and THz Waves, 2008. IRMMW-THz 2008*, Pasadena, CA, Sep. 15–19, 2008.

[38] M. Misra, K. Kotani, I. Kawayama, H. Murakami, and M. Tonouchi, "Observation of TO1 soft mode in SrTiO3 films by terahertz time domain spectroscopy," *APL*, vol. 87, p. 182909, 2005.

[39] A. Pashkin, "Terahertz spectroscopy of ferroelectrics and related materials," Ph.D. Thesis, Prague, Czech Republic, 2004.

[40] M. Gil, C. Damm, A. Giere, M. Sazegar, J. Bonache, R. Jakoby, and F. Martin, "Electrically tunable split-ring resonators at microwave frequencies based on barium-strontium-titanate thick films," *Electron. Lett.*, vol. 45, no. 8, 2009.

[41] T. H. Hand and S. A. Cummer, "Frequency tunable electromagnetic metamaterial using ferroelectric loaded split rings," *JAP*, vol. 103, p. 066105, 2008.

[42] G. Houzet, X. Melique, D. Lippens, L. Burgnies, G. Velu, and J.-C. Carru, "Microstrip transmission line loaded by split-ring resonators tuned by ferroelectric thin film," *Progr. Electromagn. Res. C*, vol. 12, pp. 225–236, 2010.

[43] Z. Qian, K. Lei, D. Bo, Z. HongJie, X. Qin, L. Bo, Z. Ji, L. L. Tu, and M. Y. Gang, "Isotropic negative permeability composite based on Mie resonance of the BST-MgO dielectric medium," *Chinese Sci. Bull.*, vol. 53, no. 21, pp. 3272–3276, Nov. 2008.

[44] F. Zhang, D. Lippens, and A. L. Borja, "Low profile small antenna using ferroelectrics cube based artificial magnetic conductor," in *2010 Proc. 4th Eur. Conf. Antennas Propag. (EuCAP)*, , Apr. 12–16, 2010, pp. 1–5.

[45] J. F. Scott, H. J. Fan, S. Kawasaki, J. Banys, M. Ivanov, A. Krotkus, J. Macutkevic, R. Blinc, V. V. Laguta, P. Cevc, J. S. Liu, and A. L. Kholkin, "Terahertz emission from tubular $Pb(Zr,Ti)O_3$ nanostructures," *Nano Lett.*, vol. 8, no. 12, pp. 4404–4409, 2008.

[46] H. L. Glass, "Ferrite films for microwave and millimeter-wave devices," *Proc. IEEE*, vol. 76, no. 2, pp. 151–158, Feb. 1988.

[47] J. D. Adam, S. V. Krishnaswami, S. H. Talisa, and K. C. Yoo, "Thin-film ferrites for microwave and millimeter-wave applications," *J. Magn. Magn. Mater.*, vol. 83, p. 419, 1990.

[48] D. B. Nicholson, "Hexagonal ferrites for millimeter-wave applications," *Hewlett-Packard J.*, vol. 41, p. 59, 1990.

[49] V. G. Harris *et al.*, "Ba-hexaferrite films for next generation microwave devices (invited)," *J. Appl. Phys.*, vol. 99, p. 08M911, 2006.

[50] A. B. Ustinov, A. S. Tatarenko, G. Srinivasan, and A. M. Balbashov, "Al substituted Ba-hexaferrite single-crystal films for millimeter-wave devices," *J. Appl. Phys.*, vol. 105, p. 023908, 2009.

[51] A. B. Ustinov and G. Srinivasan, "Subterahertz excitations and magnetoelectric effects in hexaferrite-piezoelectric bilayers," *Appl. Phys. Lett.*, vol. 93, p. 142503, 2008.

[52] M. Popov, I. Zavislyak, A. Ustinov, and G. Srinivasan, "Sub-terahertz magnetic and dielectric excitations in hexagonal ferrites," *IEEE Trans. Magn.*, vol. 47, no. 2, 2011.

[53] Y. Lu and R. J. Knize, "Realization of negative refraction via overlapping ferroelectric and ferromagnetic oxides," *Piers Online*, vol. 6, no. 3, 2010.

[54] W. J. Kim *et al.*, "Electrically and magnetically tunable microwave device using (Ba,Sr) $TiO_3/Y_3Fe_5O_{12}$ multilayer," *Appl. Phys. A: Mater. Sci. Process.*, vol. 71, p. 7, 2000.

[55] Y. K. Fetisov and G. Srinivasan, "Electrically tunable ferrite-ferroelectric microwave delay lines," *Appl. Phys. Lett.*, vol. 87, p. 103502, 2005.

[56] Y. K. Fetisov and G. Srinivasan, "Electric field tuning characteristics of a ferrite-piezoelectric microwave resonator," *Appl. Phys. Lett.*, vol. 88, p. 143503, 2006.

[57] A. B. Ustinov *et al.*, "Electric field tunable ferrite-ferroelectric hybrid wave microwave resonators: Experiment and theory," *J. Appl. Phys.*, vol. 100, p. 093905, 2006.

[58] A. B. Ustinov, B. A. Kalinikos, V. S. Tiberkevich, A. N. Slavin, and G. Srinivasan, "Q factor of dual-tunable microwave resonators based on yttrium iron garnet and barium strontium titanate layered structures," *J. Appl. Phys.*, vol. 103, p. 063908, 2008.

[59] A. B. Ustinov, G. Srinivasan, and Y. K. Fetisov, "Microwave resonators based on single-crystal yttrium iron garnet and lead magnesium niobate-lead titanate layered structures," *J. Appl. Phys.*, vol. 103, p. 063901, 2008.

[60] A. B. Ustinov, Y. K. Fetisov, and G. Srinivasan, "Planar ferrite-piezoelectric composite microwave resonator with electric and magnetic frequency tuning," *Tech. Phys. Lett.*, vol. 34, p. 593, 2008.

[61] A. S. Tatarenko, A. B. Ustinov, G. Srinivasan, V. M. Petrov, and M. I. Bichurin, "Microwave magnetoelectric effects in bilayers of piezoelectrics and ferrites with cubic magnetocrystalline anisotropy," *J. Appl. Phys.*, vol. 108, p. 063923, 2010.

[62] A. Zylbersztejn and N. F. Mott, "Metal-insulator transition in vanadium dioxide," *Phys. Rev. B Solid State*, vol. 11, pp. 4383–4395, 1975.

[63] H.-T. Chen *et al.*, "Experimental demonstration of frequency-agile terahertz metamaterials," *Nature Photon.*, vol. 2, p. 295, 2008.

[64] B. G. Chae, H. T. Kim, D. H. Youn, and K. Y. Kang, "Abrupt metal-insulator transition observed in VO2 thin films induced by a switching voltage pulse," *Physica B*, vol. 369, no. 1–4, pp. 76–80, 2005.

[65] S. Lysenko *et al.*, "Light-induced ultrafast phase transitions in VO2 thin film," *Appl. Surf. Sci.*, vol. 252, p. 5512, 2006.

[66] T. Driscoll, H. T. Kim, B. G. Chae, M. Di Ventra, and D. N. Basov, "Phase-transition driven memristive system," *Appl. Phys. Lett.*, vol. 95, p. 043503, 2009.

[67] T. Driscoll *et al.*, "Memory Metamaterials," *Science*, vol. 325, p. 1518, 2009.

[68] M. J. Dicken *et al.*, "Frequency tunable near-infrared metamaterials based on VO2 phase transition," *Opt. Express*, vol. 17, p. 18330, 2009.

[69] M. A. Seo and J. S. Kyung *et al.*, "Active terahertz nanoantennas based on VO_2 phase transition.," *Nano Lett.*, vol. 10, p. 2064, 2010.

[70] J. S. Kyung *et al.*, "Active terahertz metamaterials: Nano-slot antennas on VO2 thin films," *Phys. Status Solid. C*, vol. 8, p. 1227, 2011.

[71] S. R. Ovshinsky, "Reversible electrical switching phenomena in disordered structures," *Phys. Rev. Lett.*, vol. 21, p. 1450, 1968.

[72] N. Zheludev, "Commentary: All change please," *Nature Photon.*, vol. 1, p. 551, 2007.

[73] Z. L. Sámson *et al.*, "Metamaterial electrooptic switch of nanoscale thickness," *Appl. Phys. Lett.*, vol. 96, p. 143105, 2010.

[74] D. W. Hewak *et al.*, in *EPCOS'10*, Cambridge, 2010.

[75] Z. L. Sámson *et al.*, "Chalcogenide glasses in active plasmonics," *Phys. Status Solidi (RRL)*, vol. 4, p. 274, 2010.

[76] E. Plum *et al.*, "Metamaterials: Optical activity without chirality," *Phys. Rev. Lett.*, vol. 102, p. 113902, 2009.

[77] E. Plum *et al.*, "Towards the lasing spaser: Controlling metamaterial optical response with semiconductor quantum dots," *Opt. Express*, vol. 17, p. 8548, 2009.

[78] X. Wang, Y.-H. Ye, C. Zheng, Y. Qin, and T. J. Cui, "Tunable figure of merit for a negative-index metamaterial with a sandwich configuration," *Opt. Lett.*, vol. 34, no. 22, pp. 3568–3570, 2009.

[79] J. Han, J. Gu, X. Lu, M. He, Q. Xing, and W. Zhang, "Broadband resonant terahertz transmission in a composite metal-dielectric structure," *Opt. Express*, vol. 17, no. 19, pp. 16527–16534, 2009.

[80] P. G. de Gennes and J. Prost, *The Physics of Liquid Crystals Clarendon*. Oxford, U.K.: , 1993, p. 34.

[81] I. C. Khoo, *Liquid Crystals: Physical Properties and Nonlinear Optical Phenomena*. New York: Wiley InterScience, 1995.

[82] A. Penirschke, S. Müller, P. Scheele, C. Weil, M. Wittek, C. Hock, and R. Jakoby, "Cavity perturbation method for characterization of liquid crystals up to 35 GHz," in *Proc. 34th Eur. Microw. Conf.*, Amsterdam, The Netherlands, Oct. 2004, pp. 545–548.

[83] S. Mueller, A. Penirschke, C. Damm, P. Scheele, M. Wittek, C. Weil, and R. Jakoby, "Broad-band microwave characterization of liquid crystals using a temperature-controlled coaxial transmission line," *IEEE Trans. Microw. Theory Techn.*, vol. 53, no. 6, pp. 1937–1945, Jun. 2005.

[84] J. A. Bossard, X. Liang, L. Li, S. Yun, D. H. Werner, B. Weiner, and T. S. Mayer *et al.*, "Tunable frequency selective surfaces and negative-zero-positive index metamaterials based on liquid crystals," *IEEE Trans. Antennas Propag.*, vol. 56, no. 5, pp. 1308–1320, May 2008.

[85] I. C. Khoo, D. H. Werner, X. Liang, A. Diaz, and B. Weiner, "Nanosphere dispersed liquid crystals for tunable negative-zero-positive index of refraction in the optical and terahertz regimes," *Opt. Lett.*, vol. 31, no. 17, pp. 2592–2594, 2006.

[86] D. H. Werner, D.-H. Kwon, I. C. Khoo, A. V. Kildishev, and V. M. Shalaev, "Liquid crystal clad near-infrared metamaterials with tunable negative-zero-positive refractive indices," *Opt. Exspress*, vol. 15, no. 6, pp. 3342–3347, 2007.

[87] A. Minovich, D. N. Neshev, D. A. Powell, I. V. Shadrivov, and Y. S. Kivshar, "Tunable fishnet metamaterials infiltrated by liquid crystals," *Appl. Phys. Lett.*, vol. 96, p. 193103, 2010.

[88] Vendik, M. Odit, O. Vendik, D. Kholodnyak, S. Zubko, M. Sitnikova, P. Turalchuk, K. Zemlyakov, D. Kozlov, I. Munina, and S. Turgaliev, "Tunable metamaterials for THz electromagnetic spectrum," in *Abstracts, Days on Diffraction 2011*, Jun. 2011, pp. 177–178.

[89] *Nanostructured Metamaterials—Exchange Between Experts in Electromagnetics and Material Science*, A. F. de Baas, Ed. Luxembourg: Publ. Office of Eur. Union, 2010.

Irina B. Vendik (M'96) received the electronics engineer diploma and the candidate of Sc. (Ph.D.) degree from Leningrad Electrical Engineering Institute (now St. Petersburg Electrotechnical University), St. Petersburg, Russia, in 1959 and 1964 respectively, and the D. Sc. (Phys.) degree from A.F. Ioffe Physicotechnical Institute, St. Petersburg, Russia, in 1990.

She is currently a Professor of the Department of Microelectronics and Radio Engineering, and the Head of the Microwave Microelectronics Laboratory, St.-Petersburg Electrotechnical University. Her general research interests have been in solid state physics and microwave electronics. The last years she has been a leader of the group of the ETU involved in FP6 and FP7 projects of the EC.

Dr. Vendik is a member of EuMA since 2006. She is an honored educator of Russian Federation (1999).

Orest G. Vendik, photograph and biography not available at time of publication.

Mikhail A. Odit, photograph and biography not available at time of publication.

Dmitry V. Kholodnyak, photograph and biography not available at time of publication.

Svetlana P. Zubko, photograph and biography not available at time of publication.

Margarita F. Sitnikova, photograph and biography not available at time of publication.

Pavel A. Turalchuk, photograph and biography not available at time of publication.

Kirill N. Zemlyakov, photograph and biography not available at time of publication.

Irina V. Munina, photograph and biography not available at time of publication.

Dmitry S. Kozlov, photograph and biography not available at time of publication.

Viacheslav M. Turgaliev, photograph and biography not available at time of publication.

Alexey B. Ustinov, photograph and biography not available at time of publication.

Yeonsang Park, photograph and biography not available at time of publication.

Jinyun Kihm, photograph and biography not available at time of publication.

Chang-Won Lee, received the B.S. and M.S. degrees Seoul National University, Seoul, Korea, in 1997 and 1999, respectively, and the Ph.D. degree in 2006, at Duke University, Durham, NC, both in physics.

He joined Samsung Advanced Institute of Technology as a R&D staff member in Semiconductor Lab for research of oxide and magnetic memory devices. He is currently a senior scientist at Frontier Research Lab and working as a project leader for plasmonic metamaterial project.